Phase Diagram of P3HT/PCBM Blends and Its Implication for the Stability of Morphology

ARTICLE *in* THE JOURNAL OF PHYSICAL CHEMISTRY B · FEBRUARY 2009

Impact Factor: 3.3 · DOI: 10.1021/jp804151a · Source: PubMed

Phase Diagram of P3HT/PCBM Blends and Its Implication for the Stability of Morphology

Jun Zhao,[†] Ann Swinnen,[‡,||] Guy Van Assche,*[,†] Jean Manca,[‡,§] Dirk Vanderzande,[‡,§] and Bruno Van Mele[†]

Department of Physical Chemistry and Polymer Science, Faculty of Engineering Sciences, Vrije Universiteit Brussel, Pleinlaan 2, 1050 Brussels, Belgium, Institute for Materials Research, Hasselt University, Wetenschapspark 1, 3590 Diepenbeek, Belgium, Division IMOMEC, IMEC, Wetenschapspark 1, 3590 Diepenbeek, Belgium

Received: May 8, 2008; Revised Manuscript Received: December 8, 2008

In this work, the phase diagram of poly(3-hexyl thiophene) (P3HT) and [6,6]-phenyl C_{61}-butyric acid methyl ester (PCBM) blends is measured by means of standard and modulated temperature differential scanning calorimetry. Blends were made by solvent-casting from chlorobenzene, as blends cast from toluene or 1,2-dichlorobenzene prove to retain effects of phase segregation during casting, hindering the determination of the phase diagram. The film morphology of P3HT/PCBM blends cast from chlorobenzene results from a dual crystallization behavior, in which the crystallization of each component is hindered by the other component. A single glass transition is observed for all compositions. The glass transition temperature (T_g) increases with increasing concentration of PCBM: from 12.1 °C for pure P3HT to 131.2 °C for pure PCBM. The observed T_g defines the operating window for the thermal annealing and explains the long-term instability of both the morphology and the photovoltaic performance of the P3HT/PCBM solar cells.

Introduction

The high-performance polymer solar cells based on regioregular poly(3-hexyl thiophene) (P3HT) as donor and [6,6]-phenyl C_{61}-butyric acid methyl ester (PCBM) as acceptor represent the current state-of-the-art in organic photovoltaics.[1,2] The up-to-date highest efficiencies, around 5% for single layer devices, require an optimum bulk heterojunction morphology, consisting of a cocontinuous network with a maximum interface area and a mean domain size of 5−10 nm.[3−6] Such a morphology can be approached by postproduction thermal annealing processes, during which reorganization, aggregation, and further crystallization within the initially amorphous or nanocrystalline deposited films result in the formation of "larger" well-organized domains.[7−13] In general, the initial morphology of the deposited blend films is the result of a kinetically frozen phase separation or crystallization. Consequently, both thermodynamic and kinetic parameters are responsible for the morphology obtained.[6,14,15] Although the melting, crystallization, and glass transition of pure P3HT and the melting and crystallization of pure PCBM have been studied,[16−19] a comprehensive study of the phase behavior of the blends over the whole composition range was lacking until recently.[20−23] Nevertheless, the phase diagram is of key importance to gain a fundamental understanding and control of morphology development in said blends of donor−acceptor materials.[21] Moreover, it should be emphasized that the phase diagram is essential in the understanding of the long-term stability of the blended film morphology and consequently of the photovoltaic performance of the corresponding solar cells. It has in fact been demonstrated that long-term operation of various types of polymer/PCBM solar cells (including P3HT/PCBM) at elevated temperatures results in a significant change of the film morphology and a remarkable decrease of the photovoltaic performance.[24]

In this paper a systematic set of experiments is presented to obtain the phase diagram for P3HT/PCBM blends. It is assembled from data obtained by means of standard and modulated temperature differential scanning calorimetry (DSC and MTDSC, respectively).[25] Experimental evidence for the glass transition of pure PCBM, never reported in the literature, is given for the first time. As will be shown, knowledge about the phase diagram of these blends has important implications on the operating window for the thermal annealing and on the expected long-term thermal stability of the morphology in solar cell applications. The effect of the solvent selected for casting the blends is discussed.

Experimental Section

Materials and Sample Preparation. Mixtures with various ratios of P3HT (Merck, M_w = 35 000 g mol^{-1}, M_w/M_n = 1.8, regioregularity greater than 98.5% as determined by NMR) and PCBM (Solenne) were dissolved in chlorobenzene with a concentration of about 1 wt % and stirred overnight at 50 °C. Then the solutions were deposited by drop-casting on large glass plates in the glovebox under a nitrogen atmosphere to form films with a thickness of about 1 μm. After drying in nitrogen atmosphere at room temperature for 50 h to remove the residual solvents, the remaining solid films were scratched off the glass substrates in the powder form and collected for the DSC measurements. The blend compositions are expressed using the weight fraction of PCBM (f_w^{PCBM}). In addition to chlorobenzene, also 1,2-dichlorobenzene and toluene were used to cast blends with an f_w^{PCBM} of 62.7 wt %.

DSC and MTDSC Measurements. DSC measurements in both standard and modulated modes were made on a TA Instruments 2920 DSC equipped with an RCS cooling accessory.

* To whom correspondence should be addressed. E-mail: gvassche@vub.ac.be. Telephone: +32-2-6293277. Fax: +32-2-6293278.
[†] Vrije Universiteit Brussel.
[‡] Hasselt University.
[§] Division IMOMEC, IMEC.
[||] Present address: The Dow Chemical Company, Herbert H. Dowweg 5, Building ADD-1, 4530 Terneuzen, The Netherlands.

10.1021/jp804151a CCC: $40.75
Published on Web 01/21/2009

Indium was employed for both temperature and enthalpy calibration. The heat capacity was evaluated with respect to poly(methyl methacrylate) (PMMA) as a standard. Helium with a flux of about 50 mL min^{-1} was used as a purge gas. About 5 mg samples were sealed in perforated aluminum crucibles (Mettler, 40 μL).

For the DSC measurements, the scan rate was 10 K min^{-1}. The stay time at the lower limit temperature of −60.0 °C was 10 min, while the stay time at the upper limit temperatures of 310.0 °C was 1 min. Three heating−cooling cycles were run to see the reproducibility. The first heating curve was quite different from the subsequent two heating curves due to the complex thermal history of the as-prepared samples and their poor contact with the crucibles in the first heating, while all three cooling curves coincide well (see Figures S1 and S2 in Supporting Information). So the first cooling and the second heating were used for discussion. The melting and crystallization peaks were characterized by their peak temperatures.

For the MTDSC measurements, the modulation amplitude was 0.5 K with a period of 60 s. First, the samples were kept at 310.0 °C for 1 min. Subsequently, some samples were quenched in the DSC cell at about 100.0 K min^{-1} to −60.0 °C and then reheated to 310.0 °C at 2.5 K min^{-1} to observe the glass transition. Some pure PCBM samples were quenched to 103.1 °C and kept isothermal for 4000 min. After this physical aging, they were quenched to −60.0 °C and then heated to 310.0 °C at 2.5 K min^{-1} to see the glass transition and the enthalpic relaxation peak.

Results and Discussion

Phase transitions of the P3HT/PCBM blends drop-cast from chlorobenzene solutions are measured by means of DSC. In a previous publication, it was already shown that the obtained films after casting were homogeneous.[26] The importance of the casting solvent is illustrated in Figure 1, which shows the heat flow (HF) traces for the first cooling and the subsequent heating of blends with an f_w^{PCBM} of 62.7 wt % cast from different solvents, as well as thermograms representing the ideal addition and a simple mixture. The ideal addition is calculated as the sum of the thermograms for pure P3HT and pure PCBM as cast from chlorobenzene, weighted by their respective mass fractions in the blend. The simple mixture is a measured thermogram for a mixture of P3HT and PCBM powder (thus not cast from solvent). For the homogeneous blend obtained by casting from chlorobenzene, no clear melt crystallization peak is observed during the cooling, and only small melting peaks are observed during the heating. For blends cast from 1,2-dichlorobenzene and toluene, crystallization and melting peaks for both P3HT and PCBM are observed. In the series 1,2-dichlorobenzene → toluene → simple mixture, the melt crystallization and melting peaks get larger, sharper, and shift to higher temperature, approaching the behavior of the pure components (represented in ideal addition). The crystallization and melting behavior of the solvent-cast blends indicates that, following the sequence of chlorobenzene → 1,2-dichlorobenzene → toluene, an increasing phase segregation must have occurred during the solvent-casting of the blends. These results are in agreement with the solubility of PCBM in different solvents: 1 wt % in toluene, 4.2 wt % in chlorobenzene, and intermediate value in 1,2-dichlorobenzene.[1,18,27] Although there are clear melt crystallization and melting peaks during the first cooling and the subsequent heating of the simple mixture, both melt crystallization temperature (T_{mc}) and melting temperature (T_m) decrease slightly compared to the ideal addition, which possibly indicates

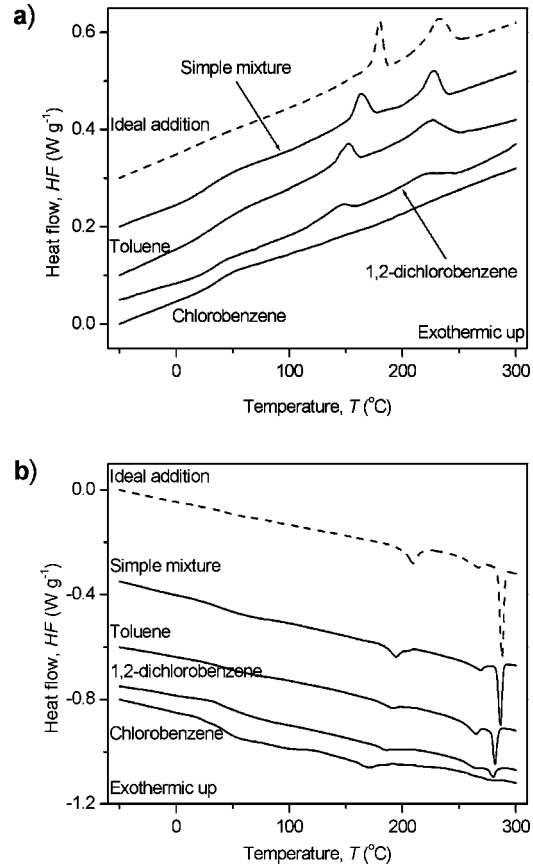

Figure 1. DSC thermograms showing HF for P3HT/PCBM blends with an f_w^{PCBM} of 62.7 wt % cast from various solvents, as indicated beside each curve: (a) the first cooling; (b) the second heating. Ideal addition represents the weighted sum of the thermograms for pure P3HT and pure PCBM. Simple mixture denotes a mixture of P3HT and PCBM powder (see text for more details). All curves are shifted vertically for clarity.

that a limited extent of mixing is achieved in the molten state due to the inherent miscibility of both components.[6,28] However, for blends that underwent a too extensive phase segregation during solvent casting from toluene and 1,2-dichlorobenzene, mixing in the liquid state through diffusion is probably too slow to achieve full mixing within a reasonable amount of time. It is worth noting that other aspects of the casting procedure, e.g., the evaporation temperature and rate, can influence the extent of phase segregation during solvent evaporation. As the films cast from chlorobenzene are homogeneous, as confirmed by Figure 1, chlorobenzene was used to study the phase diagram.

Figure 2 shows the HF traces of blends with different weight fraction of PCBM (f_w^{PCBM}). In the first cooling of pure P3HT, melt crystallization is observed as an exothermic peak with shoulder at 179.9 and 154.3 °C. In the subsequent heating, there is a melting peak at 209.5 °C followed by a shoulder at 221.2 °C. The melting enthalpy is 18.3 J g^{-1}, which corresponds to a degree of crystallinity of about 18.5% (the melting enthalpy of perfect P3HT crystals is 99.0 J g^{-1}).[29] With the addition of PCBM, both the melt crystallization peak and the melting peak of P3HT in the blends shift to lower temperatures with a smaller area and broader shape. When the f_w^{PCBM} is increased to 62.7 wt %, no melt crystallization of P3HT can be seen any more. For this composition, there are broad double melting peaks of P3HT at 170.4 and 187.2 °C with a total area of 3.2 J g^{-1}. In addition, broad double melting peaks of PCBM start to be visible at 263.6 and 280.4 °C with a total area of 0.9 J g^{-1}. With a further increase of f_w^{PCBM}, the double melting peaks of P3HT

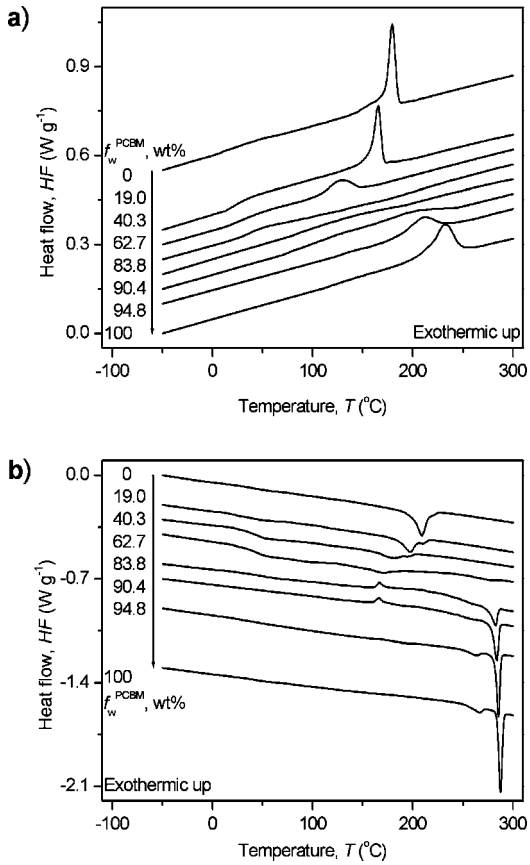

Figure 2. DSC thermograms showing HF for P3HT/PCBM blends with various compositions, as indicated beside each curve in f_w^{PCBM}: (a) the first cooling; (b) the second heating. All curves are shifted vertically for clarity.

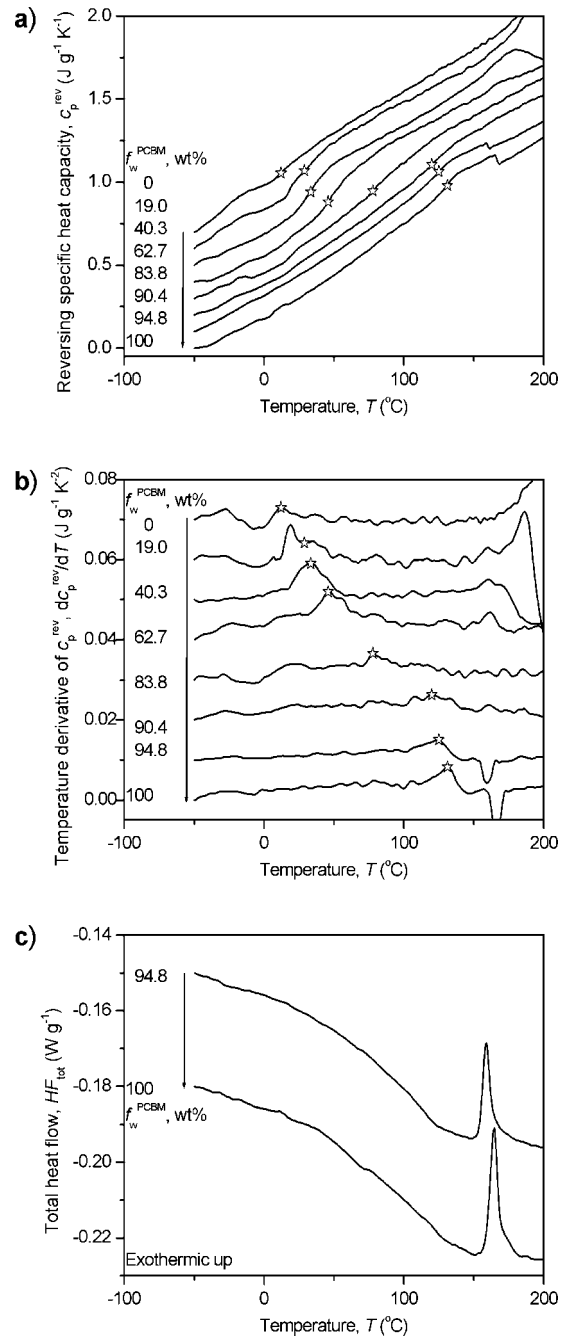

Figure 3. MTDSC thermograms showing (a) c_p^{rev}, (b) dc_p^{rev}/dT, and (c) HF_{tot} for quenched P3HT/PCBM blends with various compositions, as indicated beside each curve in f_w^{PCBM}. The open stars in parts a and b indicate the T_g. All curves are shifted vertically for clarity.

can no longer be observed, while those of PCBM shift to higher temperatures with a larger area and sharper shape. For the f_w^{PCBM} of 83.8 wt %, a broad melt crystallization peak of PCBM appears at 143.1 °C with an area of 1.9 J g^{-1}. With a further increase of f_w^{PCBM}, the peak shifts to higher temperatures with a larger area and sharper shape. A cold crystallization peak of PCBM is observed at 167.3 and 166.2 °C for the blends with an f_w^{PCBM} of 83.8 and 90.4 wt %, respectively. These two blends show very little melt crystallization in the previous cooling. For pure PCBM, the melt crystallization peak is observed at 231.8 °C with an area of 16.5 J g^{-1}, and double melting peaks are observed at 267.5 and 287.7 °C with areas of 2.1 and 13.0 J g^{-1}, respectively. To sum up, for nearly all compositions, a double melting peak is seen for either the P3HT-rich or the PCBM-rich phase, which implies that the other phase is in an amorphous or very poorly crystalline state. For the blends with an f_w^{PCBM} of 62.7 wt %, which is close to the composition that gives the highest performance of the blends,[1,2,30] the coexistence of two separate double melting peaks for both the P3HT-rich and the PCBM-rich phase can be seen.

Notwithstanding the quenching procedure, the quenched P3HT/PCBM blends are still semicrystalline, which makes the observation of glass transition difficult. Nevertheless, glass transitions can be seen more clearly by MTDSC than by DSC.[25] Figure 3 shows the evolution of the reversing specific heat capacity (c_p^{rev}) and its temperature derivative (dc_p^{rev}/dT) for quenched P3HT/PCBM blends. A single glass transition is observed for all samples, and it shifts to higher temperatures with increasing f_w^{PCBM}. The glass transition temperatures (T_g) of pure P3HT is 12.1 °C. This value is in good agreement with the well-cited value of 12 °C reported by Zhao et al.[16] A much higher value of 110 °C was also reported by Kim et al., but no clear feature of glass transition was visible in the DSC trace.[6,18]

Figure 3 also shows that pure PCBM has a T_g of 131.2 °C. Although the amorphous state of the C_{60} was reported,[31] there was no previous report of the glass transition of PCBM in the literature. For pure PCBM and the blends with an f_w^{PCBM} of 94.8 wt %, a drop in c_p^{rev} follows the glass transition. This drop is attributed to the cold crystallization, which is also observed as an exothermic peak in the total HF (HF_{tot}) (see Figure 3, part c).

To support that the step change in c_p^{rev} is indeed due to a glass transition, a further experimental evidence by means of the enthalpic relaxation behavior is shown in Figure 4.[32,33]

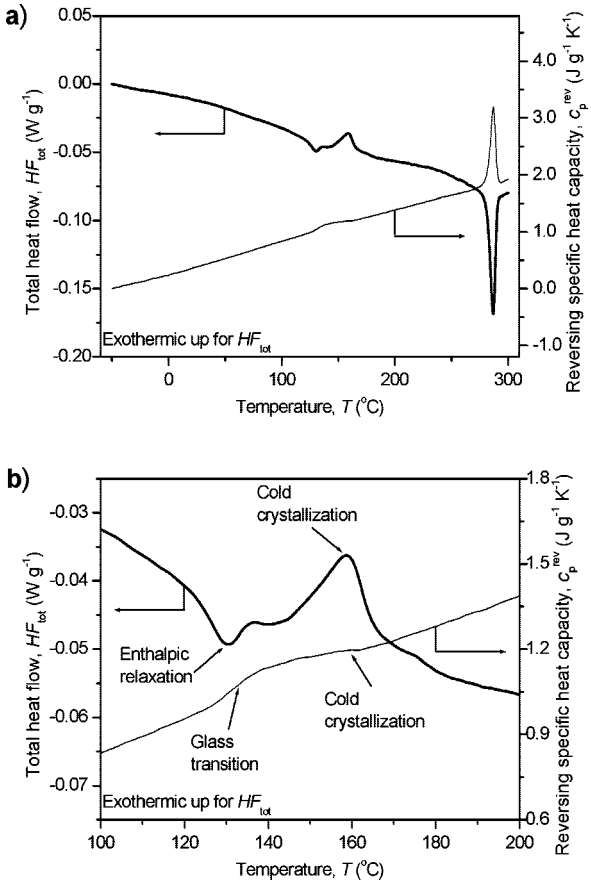

Figure 4. (a) MTDSC thermograms showing HF_{tot} and c_p^{rev} for quenched pure PCBM after physical aging at 103.1 °C for 4000 min; (b) a zoom of part a, showing the enthalpic relaxation, glass transition, and cold crystallization.

Quenched pure PCBM was physically aged at 103.1 °C for 4000 min. In the subsequent heating, an endothermic enthalpic relaxation peak of 1.6 J g^{-1} appears in HF_{tot} coinciding with a well-defined glass transition at 130.8 °C in c_p^{rev}. This enthalpic relaxation is an indicative feature that the c_p^{rev} step of pure PCBM shown in Figure 3, part a, is really a glass transition. At higher temperatures, cold crystallization is observed as an exothermic peak at 159.0 °C with an area of 5.3 J g^{-1} in HF_{tot} and as a stepwise decrease in c_p^{rev}. The big endothermic peak at 287.1 °C in both signals shown in Figure 4, part a, is the melting of PCBM.

The data obtained allow assembling a phase diagram for P3HT/PCBM blends as shown in Figure 5. During our study, no evidence of (liquid−liquid) phase separation in the molten state of P3HT and PCBM was found for blend films cast from chlorobenzene, which is, as mentioned before, a solvent that gives homogeneous P3HT/PCBM films after casting.[26] Our results indicate that these films also are (or become) homogeneous above the melting points of PCBM, which means that a full remixing of the molten phases occurs. Thus the phase morphology is the result of the (dual) crystallization behavior solely, in contrast to poly(2-methoxy-5-(3′,7′-dimethyloctyloxy)-1,4-phenylene vinylene) (MDMO-PPV)/PCBM blends, for which the phase morphology originates from the liquid−liquid phase separation due to the inherent immiscibility of the components.[14,34] Most of the current studies of P3HT/PCBM solar cells are focused on the further tuning of the morphology of pristine blends with a complex thermal history. In this respect, the phase diagram provides the operating window for the

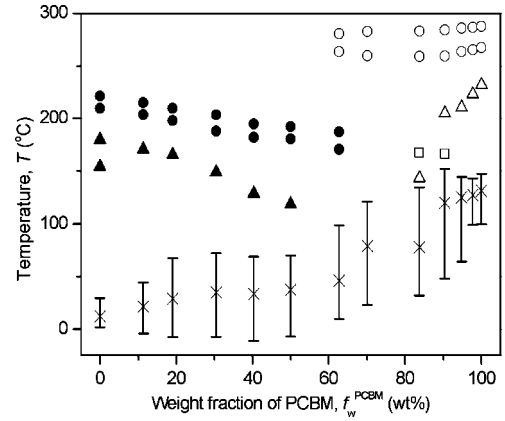

Figure 5. Phase diagram of P3HT/PCBM blends: melt crystallization temperature (▲) and melting temperature (●) of P3HT; melt crystallization temperature (Δ), cold crystallization temperature (□), and melting temperature (○) of PCBM; and T_g (×) with its range (vertical bar) of the blends. The data are obtained from Figure 2 and Figure 3, parts a and b.

annealing treatment. The lower limit of the annealing temperature is the T_g for each composition, as the mobility needed for crystallization is frozen in below the T_g. The T_g for the highest performance P3HT/PCBM blends with an f_w^{PCBM} of 45−50 wt % is less than 40 °C.[1,2,30] Consequently, annealing procedures need at least a temperature of 40 °C. However, as mobility is available above the T_g, an even more important implication is that the phase morphology of the blends will only be frozen when the T_g is above the desired maximum operating temperature of the solar cells, which can be as high as 80 °C. This means that in said conditions the morphology of P3HT/PCBM blends is fundamentally unstable. This applies as well for the morphology of the amorphous phase as for the morphology of the crystalline phase.[11,35] It has been observed that the P3HT/PCBM layers sandwiched between rigid electrodes in solar cells had a much higher stability, probably because the morphology development is slowed down.[36] However, the layers are still intrinsically unstable and they just take longer time to show the decreased performance. In the literature, two general routes have been explored to improve the thermal stability and reduce the phase separation: cross-linking and the use of compatibilizers.[37,38] According to our results, a more effective way to increase the long-term thermal stability of the phase morphology might be to replace P3HT by a polymer that is miscible with PCBM and has a higher T_g (e.g., 120 °C or above), as the T_g of PCBM is sufficiently high (131.2 °C). A preliminary work in this direction has been reported recently.[39]

Conclusions

In this work the phase diagram of P3HT and PCBM blends was measured by means of DSC and MTDSC. It is found that the film morphology of these blends results from a dual crystallization behavior in which the crystallization of each component is hindered by the other component. No indication of phase separation in the molten state of the blends is found; a single glass transition is observed for all compositions and the T_g increases with increasing concentration of PCBM. The T_g for each composition determines the lower limit of the operating window for the thermal annealing that is usually used to optimize the bulk heterojunction morphology. The phase diagram also shows that the morphology of the blends with an f_w^{PCBM} of 45−50 wt %, giving the highest performance, is intrinsically unstable at the desired maximum operating tem-

perature of 80 °C, as the T_g is less than 40 °C. As the T_g of PCBM is sufficiently high (131.2 °C), we are currently developing some high T_g alternatives to P3HT.

Acknowledgment. G. Van Assche is a Postdoctoral Fellow of the Research Foundation - Flanders (FWO - Vlaanderen). The research was partly performed in the framework of the IWT-project 030220 "Nanosolar" funded by the Institute for the Promotion of Innovation by Science and Technology in Flanders (IWT) and partly by the FWO-project G.0091.07.

Supporting Information Available: Two figures demonstrating three consecutive heating−cooling cycles of DSC measurements and the first and second heating of DSC measurements showing the effect of the solvent casting procedure. This material is available free of charge via the Internet at http://pubs.acs.org.

References and Notes

(1) Li, G.; Shrotriya, V.; Huang, J.; Yao, Y.; Moriarty, T.; Emery, K.; Yang, Y. *Nat. Mater.* **2005**, *4*, 864–868.
(2) Ma, W.; Yang, C.; Gong, X.; Lee, K.; Heeger, A. J. *Adv. Funct. Mater.* **2005**, *15*, 1617–1622.
(3) Halls, J. J. M.; Walsh, C. A.; Greenham, N. C.; Marseglia, E. A.; Friend, R. H.; Moratti, S. C.; Holmes, A. B. *Nature* **1995**, *376*, 498–500.
(4) Yu, G.; Gao, J.; Hummelen, J. C.; Wudl, F.; Heeger, A. J. *Science* **1995**, *270*, 1789–1791.
(5) Yu, G.; Heeger, A. J. *J. Appl. Phys.* **1995**, *78*, 4510–4515.
(6) Thompson, B. C.; Frechet, J. M. J. *Angew. Chem., Int. Ed.* **2008**, *47*, 58–77.
(7) Riedel, I.; Parisi, J.; Dyakonov, V.; Lutsen, L.; Vanderzande, D.; Hummelen, J. C. *Adv. Funct. Mater.* **2004**, *14*, 38–44.
(8) Yang, X.; Loos, J.; Veenstra, S. C.; Verhees, W. J. H.; Wienk, M. M.; Kroon, J. M.; Michels, M. A. J.; Janssen, R. A. J. *Nano Lett.* **2005**, *5*, 579–583.
(9) Mihailetchi, V. D.; Koster, L. J. A.; Blom, P. W. M.; Melzer, C.; de Boer, B.; van Duren, J. K. J.; Janssen, R. A. J. *Adv. Funct. Mater.* **2005**, *15*, 795–801.
(10) Riedel, I.; von Hauff, E.; Parisi, J.; Martin, N.; Giacalone, F.; Dyakonov, V. *Adv. Funct. Mater.* **2005**, *15*, 1979–1987.
(11) Swinnen, A.; Haeldermans, I.; vande Ven, M.; D'Haen, J.; Vanhoyland, G.; Aresu, S.; D'Olieslaeger, M.; Manca, J. *Adv. Funct. Mater.* **2006**, *16*, 760–765.
(12) Warman, J. M.; de Haas, M. P.; Anthopoulos, T. D.; de Leeuw, D. M. *Adv. Mater.* **2006**, *18*, 2294–2298.
(13) Loi, M. A.; Toffanin, S.; Muccini, M.; Forster, M.; Scherf, U.; Scharber, M. *Adv. Funct. Mater.* **2007**, *17*, 2111–2116.
(14) Yang, X.; Loos, J. *Macromolecules* **2007**, *40*, 1353–1362.
(15) Moule, A. J.; Meerholz, K. *Adv. Mater.* **2008**, *20*, 240–245.
(16) Zhao, Y.; Yuan, G.; Roche, P.; Leclerc, M. *Polymer* **1995**, *36*, 2211–2214.
(17) Rispens, M. T.; Meetsma, A.; Rittberger, R.; Brabec, C. J.; Sariciftci, N. S.; Hummelen, J. C. *Chem. Commun.* **2003**, *17*, 2116–2118.
(18) Kim, Y.; Choulis, S. A.; Nelson, J.; Bradley, D. D. C.; Cook, S.; Durrant, J. R. *Appl. Phys. Lett.* **2005**, *86*, 063502.
(19) Zen, A.; Saphiannikova, M.; Neher, D.; Grenzer, J.; Grigorian, S.; Pietsch, U.; Asawapirom, U.; Janietz, S.; Scherf, U.; Lieberwirth, I.; Wegner, G. *Macromolecules* **2006**, *39*, 2162–2171.
(20) Swinnen, A.; Zhao, J.; Van Assche, G.; Vanderzande, D.; D'Olieslaeger, M.; Manca, J. V.; Van Mele, B. In *Proceedings of the Society of Photo-Optical Instrumentation Engineers (SPIE) - Organic Photovoltaics VIII*; Kafafi, Z. H., Lane, P. A., Eds.; 2007; Conference on Organic Photovoltaics VIII, San Diego, CA, Aug 28−30, 2007, SPIE; Air Products & Chem. Inc., Volume *6656*, pp 65619−65619.
(21) Mueller, C.; Ferenczi, T. A. M.; Campoy-Quiles, M.; Frost, J. M.; Bradley, D. D. C.; Smith, P.; Stingelin-Stutzmann, N.; Nelson, J. *Adv. Mater.* **2008**, *20*, 3510–3515.
(22) Kim, J. Y.; Frisbie, C. D. *J. Phys. Chem. C* **2008**, *112*, 17726–17736.
(23) During the revision of this manuscript, a paper by Mueller et al.[21] was published in which the phase diagram of P3HT/PCBM blends is constructed from DSC curves of the first heating of the solvent-cast blends and in which reference is made to preliminary results presented by our group.[20] In the paper, eutectic crystallization with a peak eutectic temperature of 205 °C at the f_w^{PCBM} of 35 wt % is suggested. This interpretation is not supported by our results. From our experience, the first heating of samples cast from solvents often displays a complex thermal behavior, which is affected by, among others, the solvent, the evaporation temperature and rate, and the film thickness.
(24) Bertho, S.; Janssen, G.; Cleij, T. J.; Conings, B.; Moons, W.; Gadisa, A.; D'Haen, J.; Goovaerts, E.; Lutsen, L.; Manca, J.; Vanderzande, D. *Sol. Energy Mater. Sol. Cells* **2008**, *92*, 753–760.
(25) *Modulated-Temperature Differential Scanning Calorimetry: Theoretical and Practical Applications in Polymer Characterization*; Reading, M., Hourston, D. J., Eds.; Springer: The Netherlands, 2006.
(26) Goris, L.; Poruba, A.; Purkrt, A.; Vandewal, K.; Swinnen, A.; Haeldermans, I.; Haenen, K.; Manca, J. V.; Vanecek, M. *J. Non-Cryst. Solids* **2006**, *352*, 1656–1659.
(27) Hoppe, H.; Sariciftci, N. S. *J. Mater. Chem.* **2006**, *16*, 45–61.
(28) Yang, C.; Hu, J. G.; Heeger, A. J. *J. Am. Chem. Soc.* **2006**, *128*, 12007–12013.
(29) Malik, S.; Nandi, A. K. *J. Polym. Sci., Part B: Polym. Phys.* **2002**, *40*, 2073–2085.
(30) Reyes-Reyes, M.; Kim, K.; Carroll, D. L. *Appl. Phys. Lett.* **2005**, *87*, 083506.
(31) Gao, M.; Zhang, H. *Phys. Lett. A* **1996**, *213*, 203–206.
(32) Hutchinson, J. M. *Prog. Polym. Sci.* **1995**, *20*, 703–760.
(33) Zhao, J.; Wang, J.; Li, C.; Fan, Q. *Macromolecules* **2002**, *35*, 3097–3103.
(34) Yang, X.; van Duren, J. K. J.; Janssen, R. A. J.; Michels, M. A. J.; Loos, J. *Macromolecules* **2004**, *37*, 2151–2158.
(35) Ma, W.; Kim, J. Y.; Lee, K.; Heeger, A. J. *Macromol. Rapid Commun.* **2007**, *28*, 1776–1780.
(36) Padinger, F.; Rittberger, R. S.; Sariciftci, N. S. *Adv. Funct. Mater.* **2003**, *13*, 85–88.
(37) Drees, M.; Hoppe, H.; Winder, C.; Neugebauer, H.; Sariciftci, N. S.; Schwinger, W.; Schaeffler, F.; Topf, C.; Scharber, M. C.; Zhu, Z.; Gaudiana, R. *J. Mater. Chem.* **2005**, *15*, 5158–5163.
(38) Sivula, K.; Ball, Z. T.; Watanabe, N.; Frechet, J. M. J. *Adv. Mater.* **2006**, *18*, 206–210.
(39) Bertho, S.; Haeldermans, I.; Swinnen, A.; Moons, W.; Martens, T.; Lutsen, L.; Vanderzande, D.; Manca, J.; Senes, A.; Bonfiglio, A. *Sol. Energy Mater. Sol. Cells* **2007**, *91*, 385–389.

JP804151A